ISSN (Print) 1226-1750
ISSN (Online) 2233-6656
Journal of Magnetics 25(3), 335-340 (2020) https://doi.org/10.4283/JMAG.2020.25.3.335

A Study on the Core Loss of SPWM Inverter Drive IPMSM considering High Frequency Harmonics

Do-hyun Kim, Byeong-chul Lee, Cheon-ho Song, and Ki-chan Kim*

Department of Electrical Engineering, Hanbat National University, Daejeon 34158, Republic of Korea

(Received 1 June 2020, Received in final form 21 August 2020, Accepted 25 August 2020)

In the paper, the core loss of SPWM inverter drive IPMSM is analyzed considering high frequency harmonics caused by SPWM and field weakening control. The output current of SPWM inverter has many high frequency harmonics at the field weakening region. The high frequency harmonics would affect the core loss on each part such as the yoke, teeth, shoe, and rotor. Therefore, IPMSM core of double layer type is divided into 6 parts to analyze the core loss in each part. In order to calculate the core loss considering the harmonics, the SPWM current is required. This is extracted by linking the SPWM inverter drive IPMSM. FEM analysis is used to compare the core loss when sinusoidal current and SPWM current are applied. The result that which part of the core is most affected is analyzed by FFT analysis applying the P.U. system.

Keywords : core loss, electric vehicles, field weakening control, harmonics, IPMSM, pulse width modulation

1. Introduction

The PWM inverters are widely applied in speed control of motor devices. Sinusoidal pulse width modulation (SPWM) technique is one of the most popular PWM techniques for harmonic reduction of inverters since there are used three sine waves displaced in 120 degrees phase difference as reference signals for three phase inverters. The inverter output voltage contains the fundamental voltage, and in addition, high frequency voltage harmonics due to the used modulation technique [1-3]. Normally, the obtained results have shown that the SPWM inverters lead to heavy core losses increasing due to the eddy current increasing [4-9]. The field weakening control is used to wide driving region of interior permanent magnet synchronous motor (IPMSM). Since flux linkage is decreased by using field weakening control, hysteresis loss is decreased at the high-speed region. However, eddy current loss is proportional to the square of electrical frequency. Therefore, core loss is increased remarkably at high speed. In case of SPWM inverter drive IPMSM, the characteristics of core loss would vary due to high frequency harmonics of input source on field weakening control [10-13].

In this paper, when output current of SPWM inverter input IPMSM on field weakening control, it is analyzed for IPMSM to core loss generated by harmonics. First, the SPWM voltage waveform of the inverter model including the carrier frequency is introduced. Secondly, to analyze the core loss due to harmonic effects on any part of the core, the double layer type IPMSM core is divided into 6 parts. Finally, core loss is compared to sinusoidal currents without a PWM switching strategy using FEM analysis.

2. Analysis Model of SPWM Inverter Drive IPMSM

The application of the SPWM inverter drive IPMSM introduced in the paper is for full electric 45[CFM] drive compressor. Figure 1 shows the structure of the IPMSM applied to the full electric compressor. The IPMSM analysis model consists of 8 poles and 12 slots, with concentrated winding 47-turns wound. The rotor has a delta type shape in two layers, and the permanent magnet material is NdFeB. Analysis model is divided into 6 parts as shown in Fig. 1 to analyze the core loss caused by the influence of harmonics on any part of the core. Table 1 shows the specifications of the IPMSM and SPWM inverters. Figure 2 shows the operating characteristic curve of the analysis model.

*Corresponding author: Tel: +82-42-821-1090
Fax: +82-42-821-1088, e-mail: kckim@hanbat.ac.kr

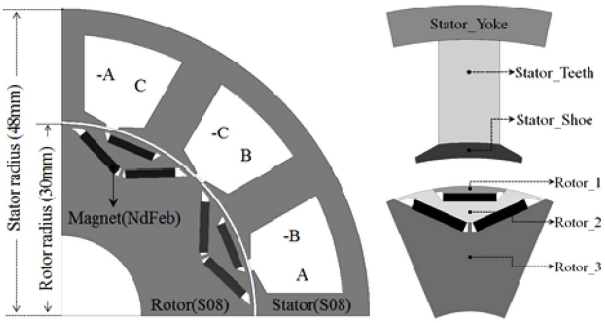

Fig. 1. FEM analysis model of IPMSM for full electric drive compressor.

Table 1. Motor and Inverter Specification for Analysis

	Parameter	Value	Unit
Motor	No. of poles	8	-
	No. of slots	12	-
	Stack length	37	mm
	Power	4.63	kW
	Torque	4.9	Nm
	Based speed	6500	rpm
	Phase resistance (R_{ph})	0.2135	ohm
	d-axis inductance (L_d)	1.5488	mH
	q-axis inductance (L_q)	2.6036	mH
Inverter	Switching frequency	10	kHz
	Battery voltage	288	V_{dc}
	Phase current	14.9	A_{rms}

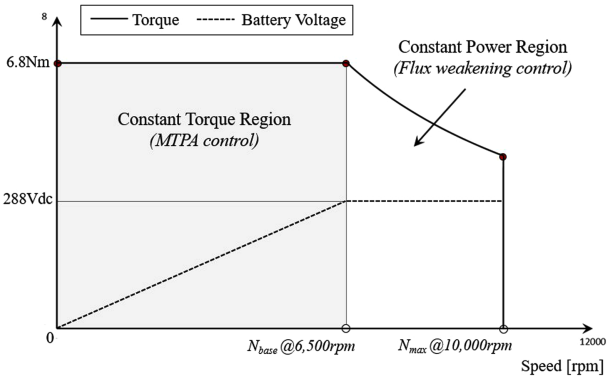

Fig. 2. Operation region of analysis model.

3. Co-simulation Model of SPWM Inverter Drive IPMSM

This chapter introduces the SPWM inverter drive IPMSM interlocking analysis model based on FEM and coupled electric circuit. The linked analysis model consists of an inverter composed of six IGBT elements, a controller for implementing the SPWM method, and a 2D

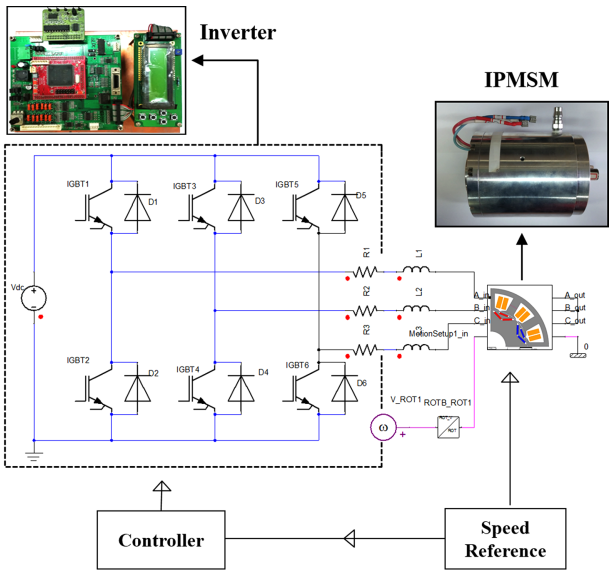

Fig. 3. (Color online) Co-simulation model of SPWM inverter drive IPMSM.

IPMSM model. In order to obtain a more accurate output current, winding resistance and leakage inductance were added between the inverter and the motor. Figure 3 shows the SPWM inverter drive IPMSM interlocking analysis model.

Used pulse width modulation to input a fixed DC voltage to the inverter. Using an inverter element, the switch is turned off and turned on repeatedly to output a controlled voltage.

Figure 4 shows a controller sub-circuit of the interlocking analysis model applying the SPWM default operating principle of Fig. 3. The switch control signal for the inverter upper bridge is determined by comparing the command voltage (V_{ref}) of each phase with the carrier wave (V_c) in real time. The PWM output signal determined in this way is used for switch control of the upper and lower parts of the inverter, thereby determining the switching operation.

4. Comparison Results on Core Loss

2.1. Comparison according to current type

Since SPWM current contains high frequency harmonics, the surface of core loss is definitely different from when sinusoidal current is applied to the input source of the motor. The core loss (P_{core}) is calculated by modified STEINMETZ method considering nth harmonics in equation (1).

$$P_{core} = \sum_{n=1} \left(K_h(B_n)(nf)B_n^{\,2} + K_c(nf, B_n)(nfB_n)^2 \right) \quad (1)$$

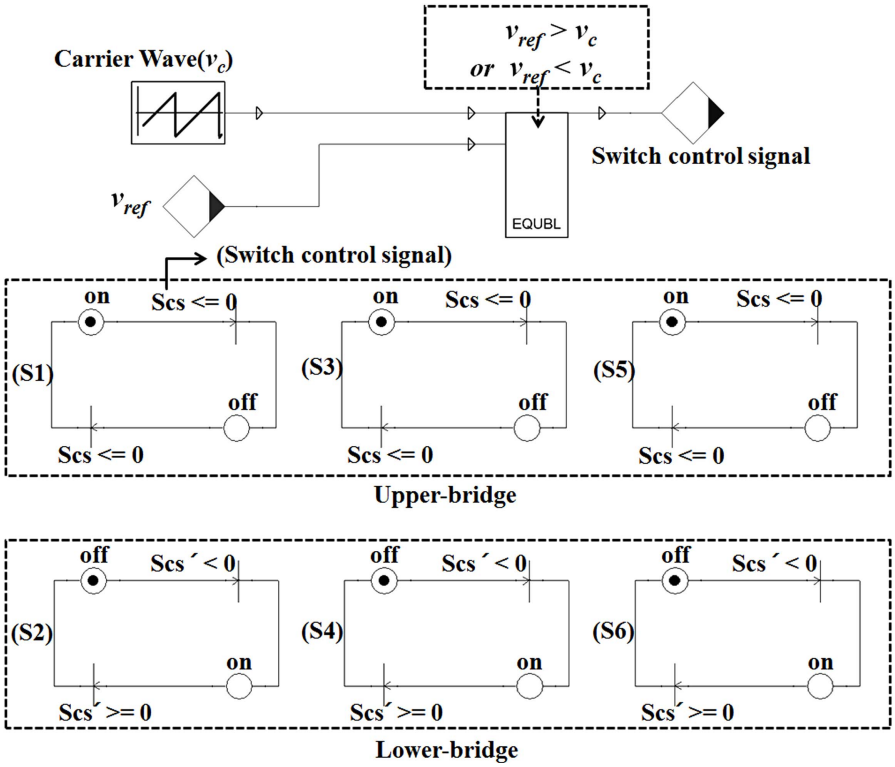

Fig. 4. SPWM Control sub-circuit in the co-simulation model.

Where f is the frequency, Bn is nth flux density and K_c, K_h denotes the coefficients of eddy-current loss and hysteresis loss. As you can see from the above formula, core loss is closely related to frequency and magnetic flux density. In the case of SPWM current, a harmonic frequency that is an integral multiple of the magnetic flux density due to the harmonic and the fundamental frequency is calculated for the core loss. Therefore, as shown in Fig. 5, it is possible to confirm that the core loss surface differs depending on the current type. Figure 6 shows a large difference in the loss waveform based on the input source in the same way as the core loss in the Magnet eddy current loss.

Figure 7 shows the core loss distribution of the IPMSM core with ideal current and SPWM current input. SPWM current expands the high core loss region due to harmonics. Especially, core loss of the teeth and yoke parts is remarkably changed.

2.2. Core loss of each part on IPMSM according to motor speed at field weakening region

Through the co-simulation for inverter drive IPMSM, the current waveform can be extracted. In order to analyze aspects of core loss caused by SPWM current on

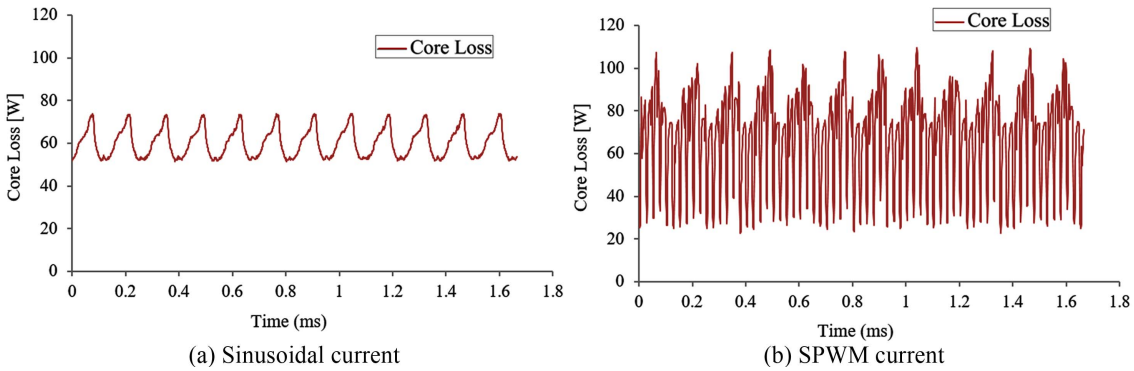

(a) Sinusoidal current (b) SPWM current

Fig. 5. (Color online) Core loss according to current type (9500 rpm).

Table 2. The core loss of each part on IPMSM by FEM analysis

Speed [rpm]	Type of current	Core loss of stator			Core loss of rotor			Total core loss	Unit
		Yoke	Teeth	Shoe	Rotor_1	Rotor_2	Rotor_3		
7500	Sinusoidal	23.09	20.13	10.42	1.49	4.53	1.69	61.35	[W]
	SPWM	24.47	21.89	10.94	1.49	4.84	2.20	65.84	[W]
	Rate of change	5.99	8.78	4.98	0.00	6.77	30.78	7.33	[%]
8500	Sinusoidal	20.79	19.73	12.45	1.55	5.72	2.21	62.45	[W]
	SPWM	24.35	23.35	13.74	1.61	6.19	3.12	72.36	[W]
	Rate of change	17.15	18.31	10.36	4.30	8.17	41.44	15.88	[%]
9500	Sinusoidal	19.45	19.34	15.01	1.65	7.29	2.82	65.55	[W]
	SPWM	24.66	24.46	16.88	1.71	8.02	4.06	79.79	[W]
	Rate of change	26.79	26.46	12.49	4.14	10.01	43.95	21.72	[%]

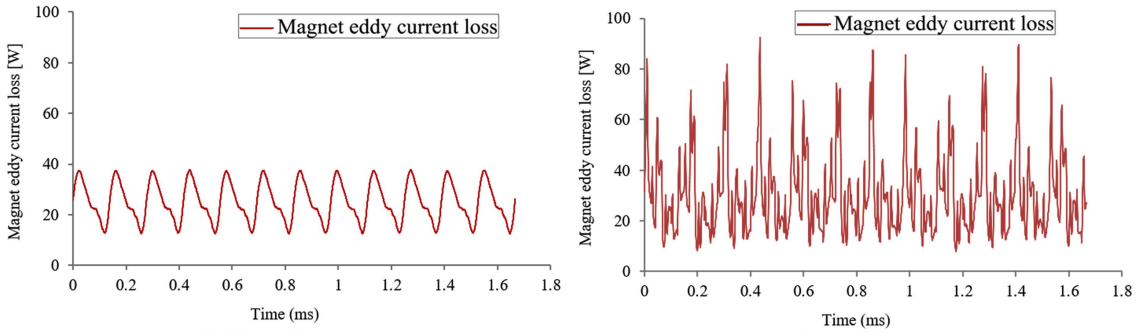

(a) Sinusoidal current (b) SPWM current

Fig. 6. (Color online) Magnet eddy current loss according to current type (9500 rpm).

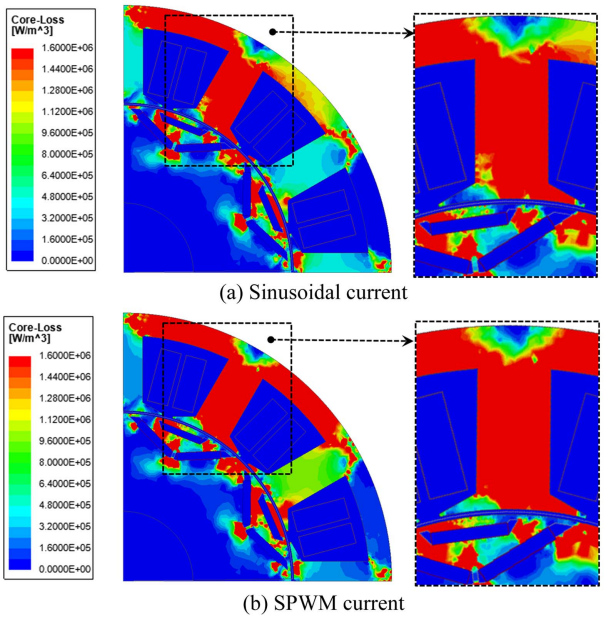

(a) Sinusoidal current

(b) SPWM current

Fig. 7. (Color online) Core loss distribution according to current type.

each part of the core, FEM analysis is conducted by comparing SPWM current with sinusoidal current at field weakening region (at 7500[rpm], 8500[rpm], 9500[rpm]).

Table 2 shows the core loss of each part on IPMSM by FEM analysis. Total core loss caused by SPWM current is generally more than the core loss by sinusoidal current due to harmonics. Core loss of rotor is very small on total core loss. Thus, the high frequency harmonics hardly affect the core loss of rotor. If the sinusoidal current or SPWM current are used as the input source, there are some different aspect of core loss according to the speeds. It could be divided into two parts. First, in case of the sinusoidal current, the core loss of the yoke and the teeth are decreased by speeding up driving because the flux density would be decreased. As can be seen from Fig. 8, it can be confirmed that the magnetic flux density generated in the core by the field weakening control decreases as the speed increases. Since the core loss hysteresis and eddy current loss are all proportional to the square of the magnetic flux density, the above-mentioned aspect is shown.

Contrastively, SPWM current has the core loss to be increased because it has high frequency harmonics. Although the magnetic flux density is lowered by the field weakening control, the frequency of the equation (1) is multiplied by the harmonic order integer multiple of the

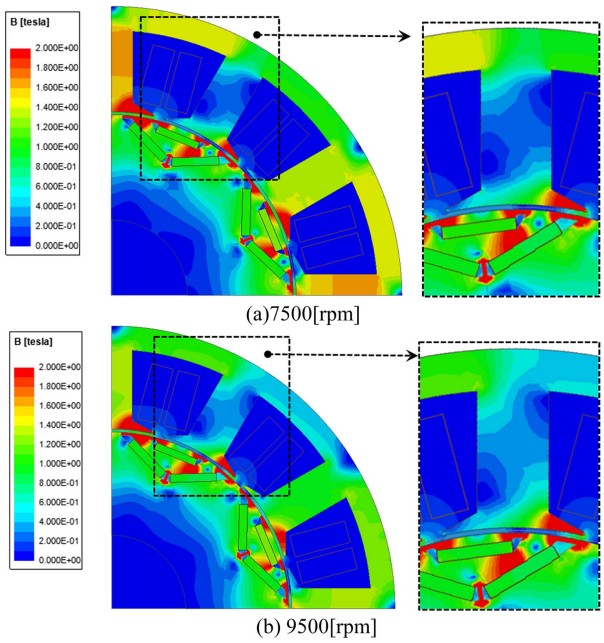

Fig. 8. (Color online) Flux density distribution according to motor speed at field weakening region.

fundamental frequency, and thus is more dominant in frequency than the magnetic flux density. Therefore, the ideal current and clearly other aspects are shown. Since the shoe part has a magnetic saturation, the flux density would not be decreased at field weakening region. Therefore, Since the core loss of the shoe part is related only to the frequency when the speed increases, the core loss of shoe part is increased according to increase the rotor speed regardless of the current type. The core loss change of the yoke part caused by sinusoidal and SPWM current is the most as the speed increases. It means that the yoke part among the 6 parts is most dominated about influence of high frequency harmonics on core loss.

In order to analysis the most dominated part of the core about high frequency harmonics, FFT analysis is conducted for each part of the core. Figure 9 shows harmonics on the core loss of shoe and yoke part by FFT analysis. Since the core loss of each part is different, Per Unit (P.U.) system is used to quantify the harmonic magnitude of core loss in each part of the core. As a result of Fig. 9, in the case of the yoke part, most harmonics are present at higher orders than the 30th harmonic. But than, the shoe part has almost no higher-order harmonics than the 50th harmonics. In the case of the shoe part, it can be seen that the 11th harmonic is displayed most clearly and the magnitude of the harmonic decreases as the speed increases. On the other hand, in the case of the yoke part, the 34th harmonic is the largest, but it can be seen that the

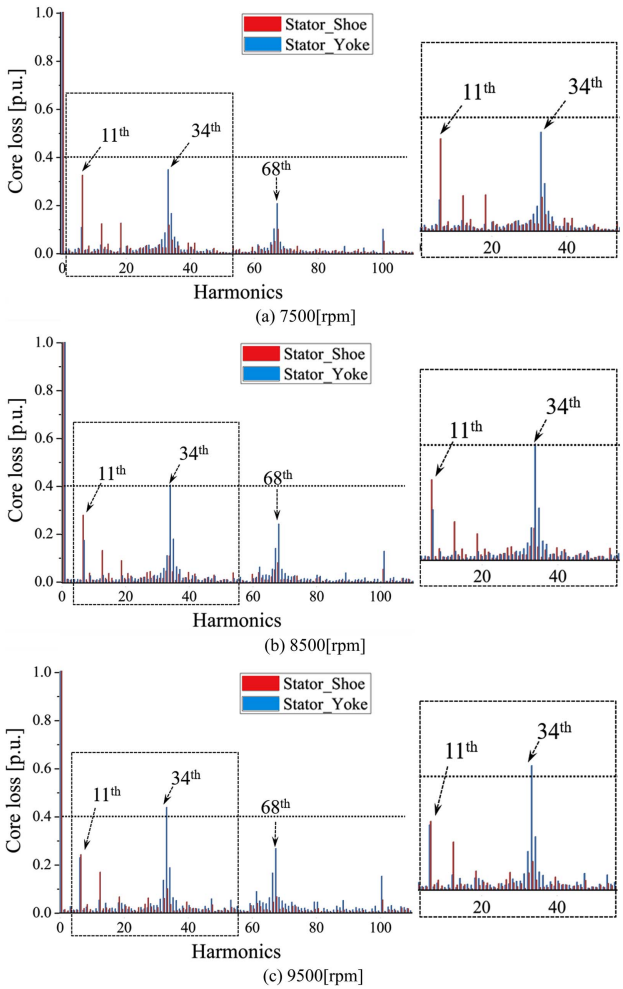

Fig. 9. (Color online) Harmonics of core loss on shoe and yoke parts by SPWM current according to motor speed.

Table 3. THD Results according to motor speed

Speed [rpm]	Section	THD [%]	Fundamental Core loss [W]	Harmonic Core loss [W]
7500	Yoke	52.80	24.37	12.87
	Teeth	56.05	21.79	12.22
	Shoe	42.25	1.74	0.74
8500	Yoke	63.55	24.20	15.38
	Teeth	63.40	23.23	14.73
	Shoe	40.20	13.73	5.52
9500	Yoke	71.94	24.49	17.62
	Teeth	69.99	24.32	17.02
	Shoe	36.60	16.87	6.18

magnitude of the harmonic increases as the speed increases.

Table 3 shows the total harmonic distortion result of the core loss for each part of the Stator core. As you can see from the FFT results with the P.U. system, Yoke and

Teeth THD increase, but Shoe THD decreases as the speed increases.

5. Conclusion

In this paper, the core loss of SPWM inverter drive IPMSM is analyzed considering high frequency harmonics caused by SPWM and field weakening control. In case of the sinusoidal current, the core loss of the yoke and the teeth are decreased by speeding up driving. On the contrary, the result in increased core loss of the yoke and teeth could be confirmed by high frequency harmonics. As a result of the FFT analysis by applying the P.U. system, yoke and teeth part of stator core is confirmed that the most affected by the high frequency harmonics.

Acknowledgment

This research was supported by the research fund of Hanbat National University in 2019.

References

[1] A. Boglietti, A. Cavagnino, M. Lazzari, and M. Pastorelli, IEEE-IEMDC2001, **17**, 20 (2001).
[2] Gabriele Grandi, Jelena Loncarski, and Obrad Dordevic, IEEE Trans. Ind. Electron. **62**, 5 (2015).
[3] John Salmon, Jeffrey Ewanchuk, and Andrew M. Knight, IEEE . Ind. Appl. **45**, 6 (2009).
[4] B. H. Lee, S. O. Kwon, Tao Sun, J. P. Hong, G. H. Lee, and H. Jin, IEEE Trans. Magn. **47**, 5 (2011).
[5] T. C. Jeong, W. H. Kim, M. J. Kim, K. D. Lee, J. J. Lee, J. H. Han, T. H. Sung, H. J. Kim, J. Lee, IEEE Trans. Magn. **49**, 5 (2013).
[6] R. Kaczmarek and M. Amar, IEEE Trans. Magn. **31**, 5 (1995).
[7] P. J. Leonard, P. Marketos, A. J. Moses, and M. Lu, IEEE Trans. Magn. **42**, 4 (2006).
[8] Katsumi Yamazaki, Masayuki Shina, Masashi Miwa, and Jun Hagiwara, IEEE Trans. Magn. **44**, 11 (2008).
[9] Shotaro Okamoto, Nicolas Denis, Yoshiyuki Kato, Masaharu Ieki, and Keisuke Fujisaki, IEEE Trans. Ind. Appl. **52**, 3 (2016).
[10] Y. Aoyama, K. Miyata, and K. Ohashi, IEEE Trans. Magn. **41**, 10 (2005).
[11] Liang Chen, David Hopkinson, Jiabin Wang, Andrew Cockburn, Martin Sparkes, and William O'Neill, IEEE Trans. Magn. **51**, 11 (2015).
[12] M. J. Kim, S. Y. Cho, K. D. Lee, J. J. Lee, J. H. Han, T. C. Jeong, W. H. Kim, D. H. Koo, and J. Lee, IEEE Trans. Magn. **49**, 7 (2013).
[13] Wenyi Liang, Patrick Chi-Kwong Luk, and Weizhong Fei, IEEE Trans. Power Electron. **33**, 4 (2018).